14th International Conference on Structural Safety and Reliability - ICOSSAR'25
1-6 June, 2025 - Los Angeles California, USA
R. Ghanem, E. Johnson, S. Masri and A. Olivier (Eds)

SEISMIC DEMAND ASSESSMENT OF DETERIORATING HIGHWAY BRIDGES UNDER EARTHQUAKE INDUCED LANDSLIDES

NOUMAN AIJAZ[1] AND JAYADIPTA GHOSH[2]

[1]Department of Civil Engineering, Indian Institute of Technology Bombay
Powai, Mumbai 400 076, Maharashtra, India
nouman@iitb.ac.in

[2]Department of Civil Engineering, Indian Institute of Technology Bombay
Powai, Mumbai 400 076, Maharashtra, India
jghosh@iitb.ac.in and https://www.civil.iitb.ac.in/faculty/details/prof-jayadipta-ghosh

Key words: Seismic Response Assessment, Earthquake-Induced Landslides, Multi-Hazard Bridge Performance, Highway Bridges, Corrosion Deterioration.

1 INTRODUCTION

Highway bridges are critical components of transportation networks in hill slopes that facilitate the movement of people and goods across the terrain. However, these vital structures face numerous challenges, particularly in hilly areas that are prone to seismic activity, landslides, and environmental deterioration such as corrosion. The combined impact of these hazards poses a significant risk to bridge integrity, potentially leading to transportation disruptions, economic losses, and public safety threats. Historical records and post-event surveys have highlighted the severe damage inflicted on bridges by earthquakes and the subsequent landslides that follow. Studies following events like the Wenchuan earthquake in 2008 [1] and the Kashmir earthquake in 2005 [2] underscore the destructive potential of flow-type landslides, characterized by rapidly moving mixtures of sediment and water, on infrastructure [3]. These events revealed that a substantial proportion of bridge failures can be directly attributed to landslides triggered by seismic activity [4].

Several studies have assessed seismic landslide hazards and analyzed slope instability triggered by earthquakes. Haugen and Kaynia [5] evaluated damage in low-rise buildings from due to flow type landslide. Jakob et al. [6] introduced a novel Intensity Measure combining debris flow velocity and depth. Similarly, other studies primarily focus on slow-moving landslides affecting buildings [7–10]. Recently, Pang et al. [4] introduced a probabilistic method for evaluating the performance of highway bridges subjected to the simultaneous impact of earthquakes and seismically triggered flow-type landslides. In addition to intermittent natural calamities, corrosion in adverse environments further weaken bridges, increasing their vulnerability to seismic events and landslides [11]. Among the various forms of deterioration, chloride-induced corrosion is a primary contributor to the structural degradation of reinforced concrete bridges [12] and has gained increased attention over the years.

Traditional deterministic approaches to bridge design often overlook the complexity of multiple hazards and structural degradation. This study addresses this gap by presenting a holistic approach to assess the seismic response of deteriorating highway bridges under the

combined effects of earthquake-induced flow-type landslides and corrosion deterioration. By integrating non-linear modelling techniques with probabilistic methods, the framework aims to provide a robust understanding of bridge performance under varying levels of deterioration and seismic loading conditions. The paper is arranged as follows. First, the proposed methodology is described, detailing four key stages: run-out analysis of flow-type landslides, slope failure probability estimation, nonlinear time history analysis of the bridge model with various corrosion levels, and the development of a probabilistic seismic demand models (PSDMs). Next, the framework is demonstrated through a case-study of example of an aging highway bridge in the Himalayan region of India under simultaneous seismic and landslide events. The results and discussion section illustrate the outcomes for various scenarios, including earthquake-only, combined earthquake and landslide, and different corrosion levels. Finally, the conclusions summarize the key findings and their implications for seismic response assessment.

2 METHODOLOGY FOR EVALUATING RESPONSE OF DETERIORATING BRIDGE UNDER COMBINED EARTHQUAKE AND LANDSLIDE LOADING

The proposed methodology includes run-out analysis to estimate the velocity and depth of landslide debris flow, followed by a landslide hazard analysis using the displacement method to determine slope failure probability. Next, a nonlinear time history analysis of the bridge model is performed, considering varying corrosion levels and landslide impact. Finally, a probabilistic seismic demand model (PSDM) is developed based on slope failure probability. The following sections outline the framework in detail.

2.1 Run-out Analysis

The proposed methodology starts with a run-out analysis to replicate the dynamic behavior of landslides. Computational fluid dynamics (CFD) using ANSYS Fluent [13] is employed to predict debris flow depth and velocity at the bridge site. A Bingham fluid model (Equation 1) is adopted, following previous studies [14,15], with a dynamic viscosity η of 10 Pa-s and yield stress τ_y of 100 Pa [16] to represent the flow behavior of the landslide.

$$\tau = \tau_y + \eta\dot{\gamma} \tag{1}$$

where, τ is the shear stress and $\dot{\gamma}$ is the rate of shear strain.

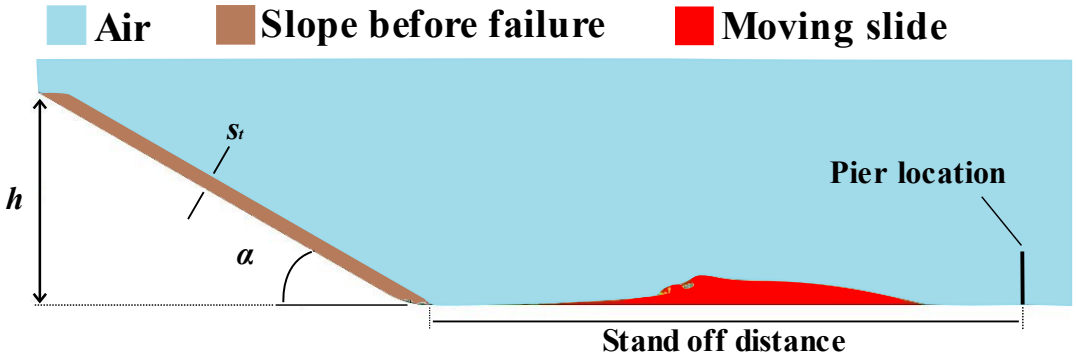

Figure 1: 2D finite element model of landslide.

Figure 1 shows the general landslide profile used in the CFD analysis. To capture uncertainties, key parameters such as slope angle (α), landslide height (h), failure slab thickness (s_t), and flow density (ρ) are varied based on the distributions in Table 1. Twenty profiles are generated using Latin Hypercube Sampling, ensuring a broad representation of potential scenarios. Assuming the stand-off distance of 500 m from the landslide trigger location to the bridge site, the flow depth and velocities are obtained from the analysis. A regression model is then fitted to the flow data to enable predictions across a wider range of landslide conditions.

Using hydraulic models from previous studies [3,17], the impact pressure exerted by the flow on the bridge pier is calculated as:

$$p_{\max} = k\rho v^2 \tag{2}$$

where, ρ is the flow density in kg/m^3, v is the impact flow velocity in m/s, and k depends on the flow type and is given as:

$$k = a \times F_r^{\,b} \tag{3}$$

$$F_r = \frac{v}{\sqrt{gh}} \tag{4}$$

where, h is the depth of flow, a and b are the empirical factors, and F_r is the Froude number. For this study, values of a and b are taken as 5.2 and -1.6, respectively [3]. Once the impact pressure is determined, the next step involves analyzing the probability of slope failure.

2.2 Probability of Slope Failure

Several methods have been developed to assess the risk of seismic-induced landslide by estimating slope displacement and correlating it with slope characteristics. Newmark [18] introduced a displacement-based approach, modeling landslides as rigid blocks sliding on an inclined plane when seismic forces exceed resistance. This method, known as Newmark displacement analysis, forms the basis for simplified predictive models. To enhance practicality, regression-based models were later introduced, including the equation by Jibson [19], adopted in this study for its inclusion of both peak ground acceleration and ground motion duration. Although Newmark displacement does not directly represent actual slope movements, the likelihood of slope failure P_f (Equation 5), derived from the predicted Newmark displacement D_n, establishes a relationship between the modeled displacement and the actual performance of the slope in the field [20].

$$P_f = 0.335\left[1 - \exp\left(-0.048 D_n^{1.565}\right)\right] \tag{5}$$

Following the computation of the probability of slope failure corresponding to a particular landslide profile and ground motion, the next step involves performing a nonlinear time-history analysis of a bridge pier considering landslide pressure.

2.3 Combined Nonlinear Time-History Analysis

After estimating landslide impact pressure and slope failure probability, nonlinear time history analysis (NLTHA) is performed in OpenSees [21] by applying ground motions followed

by dynamic landslide loading, as shown in Figure 2. A 10-second gap is introduced between the two loadings for the transient analysis to stabilize. The landslide pressure lasts 6 seconds, with a 1-second rise and 5-second decay, based on prior studies [22].

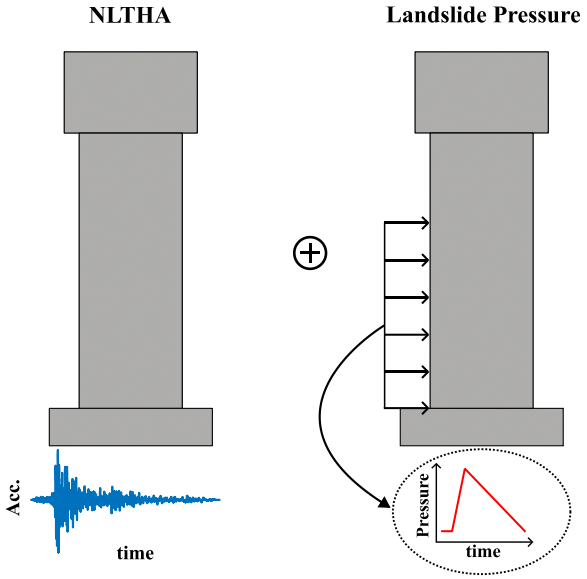

Figure 2: Combined nonlinear time-history analysis on the bridge pier.

Initially, the entirety of the landslide load is applied after each ground motion, which does not reflect real conditions since not all instances of seismic shaking triggers a landslide. To address this, displacement-based landslide analysis is used to assign slope failure probabilities for each ground motion and landslide profile, as previously discussed. Alongside the as-built model, corroded models representing different bridge condition at different points along the service lives are also analyzed, detailed in the next section.

2.4 Deterioration Modelling

Bridges made of reinforced concrete that are exposed to severe environmental conditions often experience degradation in various forms. One of these degradation mechanisms, chloride-induced corrosion, has become a growing concern [23] and hence considered in this study. The continuous corrosion of many bridge components, including the piers, significantly impacts the seismic response throughout their expected lifespan [11].

$$T_I = \frac{X^2}{4D_c}\left[erf^{-1}\left(\frac{C_0 - C_{cr}}{C_0}\right)\right]^{-2} \tag{6}$$

Equation 6 estimates the corrosion initiation time (T_I) in years, based on concrete cover X, diffusion coefficient D_c, surface chloride concentration C_o, and critical threshold C_{cr}. As indicated in Equation 6, four stochastic variables (X, D_c, C_o, C_{cr}) influence corrosion initiation time, and these values may exhibit significant variations across different bridge structures [24].

During corrosion propagation, strength loss may be primarily attributed to the reduction in the reinforcement's cross-sectional area. For bars with equal diameter and simultaneous corrosion initiation, the time-dependent steel area is expressed as:

$$A(t) = \begin{cases} nD_i^2 \dfrac{\pi}{4} & for\ t \le T_I \\ n(D(t))^2 \dfrac{\pi}{4} & for\ T_I < t < T_I + \dfrac{D_i}{0.0203 \times i_{corr}} \\ 0 & for\ t \ge T_I + \dfrac{D_i}{0.0203 \times i_{corr}} \end{cases} \tag{7}$$

where, n is the number of bars, D_i the initial diameter of bars, t the elapsed time, T_I the corrosion initiation time from Equation 6, i_{corr} denotes the corrosion rate parameter, and

$$D(t) = D_i - (0.0203 \times i_{corr} \times (t - T_I)) \tag{8}$$

It is worth noting that the corrosion rate, denoted as r_{corr}, can be represented as:

$$r_{corr} = 0.0203 \times i_{corr} \tag{9}$$

After incorporating corrosion deterioration in the bridge model and performing the NLTHA, Probabilistic Seismic Demand Models are developed using the cloud analysis approach.

2.5 Development of Seismic Demand Models

Probabilistic Seismic Demand Models (PSDMs) are developed by establishing a relationship between the Engineering Demand Parameter (EDP)—displacement ductility (μ_Δ)—and the Intensity Measure (*IM*). The cloud analysis approach is used, assuming a log-linear form to estimate median ($\mu_\Delta(t)$) and dispersion ($\beta(t)$) at any time via logarithmic regression [25]:

$$\ln(\mu_\Delta(t)) = a_o(t) + b_o(t)\ln(IM) \tag{10}$$

$$\beta(t) = \sqrt{\frac{\sum_{i=1}^{n}\left[\ln\left(EDP_i(t)\right) - \left(a_o(t) + b_o(t)\ln\left(IM_i\right)\right)\right]}{n-2}} \tag{11}$$

Here, t is the elapsed time, $a_o(t)$ and $b_o(t)$ are regression coefficients, and n is the number of ground motion. $EDP_i(t)$ reflects the peak seismic response from the NLTHA of the i^{th} ground motion with intensity IM_i.

To account for multi-hazard effects, a modified PSDM is developed by incorporating slope failure probability. This improves demand estimates and identifies threshold IMs where landslide forces become significant. At any time instant NLTHAs are performed for both earthquake-only and combined earthquake–landslide loading, generating two response clouds for each deterioration level. The slope failure probability P_f^i, for each ground motion is used to combine these responses:

$$EDP_i = P_f^i \times EDP_{i,2} + (1 - P_f^i) \times EDP_{i,1} \tag{12}$$

where, $EDP_{i,1}$ corresponds to earthquake-only loading and $EDP_{i,2}$ to combined loading. This incorporation provides a more realistic prediction of structural performance under multi-hazard loading. The next section presents a case-study of an aging highway bridge incorporating corrosion effects due to chloride-induced deterioration.

3 CASE-STUDY EXAMPLE

The proposed methodology is demonstrated on a representative case-study example bridge is assumed to be situated in the Himalayan region of India; an area characterized by active seismicity. This region has historically experienced several major earthquakes and is also prone to landslides [26].

3.1 Bridge Description and Deterioration Modelling

The impact of combined seismic and landslide loading is illustrated using a typical two-span single-pier semi-integral bridge model adopted from Shekhar et al. [27]. In this configuration, the bridge deck spans continuously over the intermediate pier and is supported by bearings at the abutments. Figure 3 shows the general layout, featuring two 20-meter spans and a 7.5-meter-wide two-lane deck and finite element model of bridge pier developed in OpenSees. The design concrete strengths are 35 MPa for the substructure and 40 MPa for the superstructure, resulting in a gravitational load of P = 3500 kN on the pier. The pier is 1.4 meters in diameter, reinforced with 24 longitudinal 32-mm bars and 16-mm transverse stirrups at 75 mm spacing. *nonlinearBeamColumn* element is used to modeled the bridge pier with *zeroLength* shear element to simulate different failure modes like flexure-shear and shear. In addition to the as-built model, the analysis includes corroded bridge models at 25, 50, and 75 years of service. The reduction in rebar area is computed using Equation 7, which depends on the corrosion initiation time and corrosion rate. As per Equation 6, the initiation time is influenced by four stochastic variables: X, D_c, C_o, and C_{cr}. Since the corrosion rate varies by location and significantly impacts area loss, three levels—low, medium, and high—are considered [24].

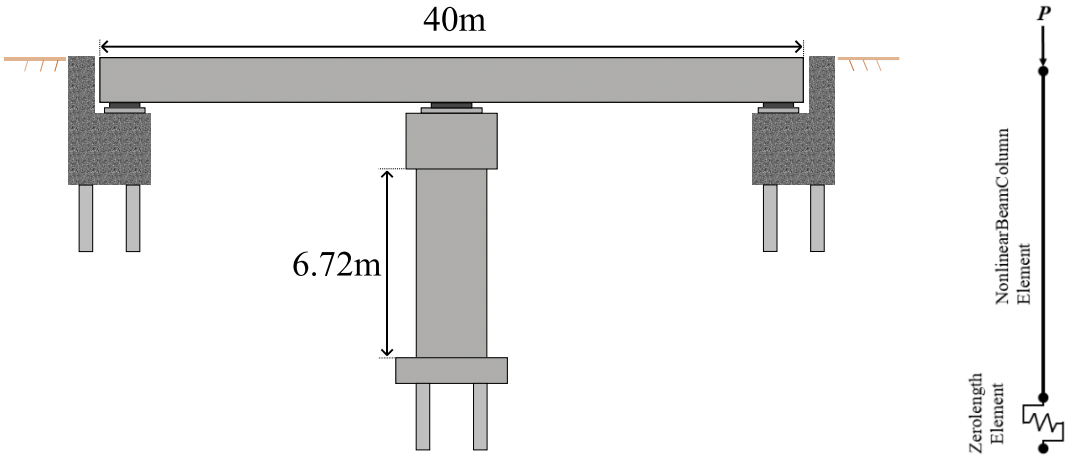

Figure 3: Case-study bridge layout along with the finite element model.

3.2 Uncertainty Modelling and Ground Motion Selection

Uncertainty in the structural response assessment may stem from variability in record-to-record uncertainty, material parameter uncertainty, deterioration uncertainty, and landslide profile uncertainty. Record-to-record uncertainty arises because the structural response under any two ground motions may not the same. To account for the variability, a suite of 90 ground motions with diverse magnitudes, source-to-site distances, and PGA values (ranging from 0.04g

to 0.83g), is adopted from Shekhar et al. [27].

Uncertainty in material properties, such as concrete and steel strengths, and deterioration parameters like corrosion initiation and rate significantly influence bridge vulnerability. Additionally, variability in landslide profiles introduces uncertainty in landslide intensity, affecting bridge response. All material parameter uncertainties used in this study are listed in Table 1. Latin Hypercube Sampling is used to generate probabilistic finite element models using the mean values and variability of these parameters for the case-study bridge. Ninety statistically distinct yet structurally identical bridge models are generated to match the number of ground motions in the suite. These models are randomly paired with ground motion time-history records. NLTHA is then performed for each pair, followed by 200 landslide intensities, recording peak displacement ductility (μ_Δ) to establish the EDP–IM relationship. Subsequently, PSDMs are developed for each bridge model to estimate the median seismic demand.

Table 1: Uncertainty Parameters for landslide profile and corrosion modelling

Parameter		Mean	CoV	Distribution
Slope angle α		23°	24	Normal
Slope height h (m)		90	20	Lognormal
Density of slope material ρ (kg/m^3)		1800	3	Normal
Failure slab thickness s_t (m)		3	45	Lognormal
Cover depth X (cm)		4.0	0.20	Lognormal
Diffusion coefficient D_c (cm^2/year)		1.29	0.10	Lognormal
Surface chloride concentration C_o (wt % concrete)		0.10	0.10	Lognormal
Critical chloride concentration C_{cr} (wt % concrete)		0.04	0.10	Lognormal
Corrosion rate (mm/year)	$r_{corr,\,low}$	0.013	0.30	Lognormal
	$r_{corr,\,med}$	0.076	0.30	Lognormal
	$r_{corr,\,high}$	0.254	0.30	Lognormal

4 RESULTS AND DISCUSSION

The results section first illustrates the hysteretic response comparison for a particular ground motion followed by one landslide pressure. Next, the response cloud for varying earthquake and landslide intensities is presented. Finally, PSDMs are developed at a specific landslide intensity for different scenarios: earthquake-only, combined earthquake and landslide, and varying aging conditions.

4.1 Hysteretic response comparison

Figures 4(a) and 4(b) illustrate the hysteretic response of the bridge under a ground motion with a PGA of 0.51g, considering varying corrosion rates and the effect of landslide loading. As corrosion increases, the force-resisting capacity of the column reduces, leading to larger displacements at the same force level, indicating reduced structural integrity. When landslide forces are included, the response amplifies in the direction of the unidirectional loading. For medium and high corrosion rates, the bridge model fails in flexure-shear mode, highlighting the critical impact of combined loading and deterioration. These results underscore the importance of accounting for both seismic and landslide hazards in the assessment and design of aging bridges.

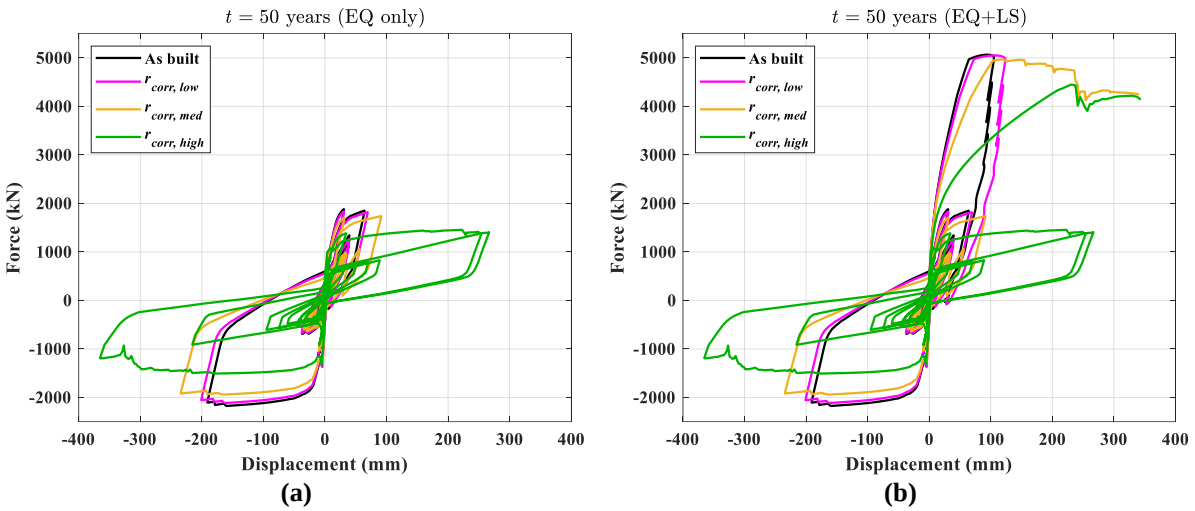

Figure 4: Hysteretic response comparison at t = 50 year for; (a) Earthquake only; and (b) Combined earthquake and landslide load.

4.2 Development of modified PSDM for non-corroded case

Figure 5 shows the bridge pier response across varying earthquake and landslide intensities. Two regions are evident: one dominated by seismic forces at lower landslide intensities, and another where landslide pressures govern the peak response as intensity increases. A specific landslide intensity is then selected (highlighted in red in Figure 5) for developing PSDMs across all scenarios.

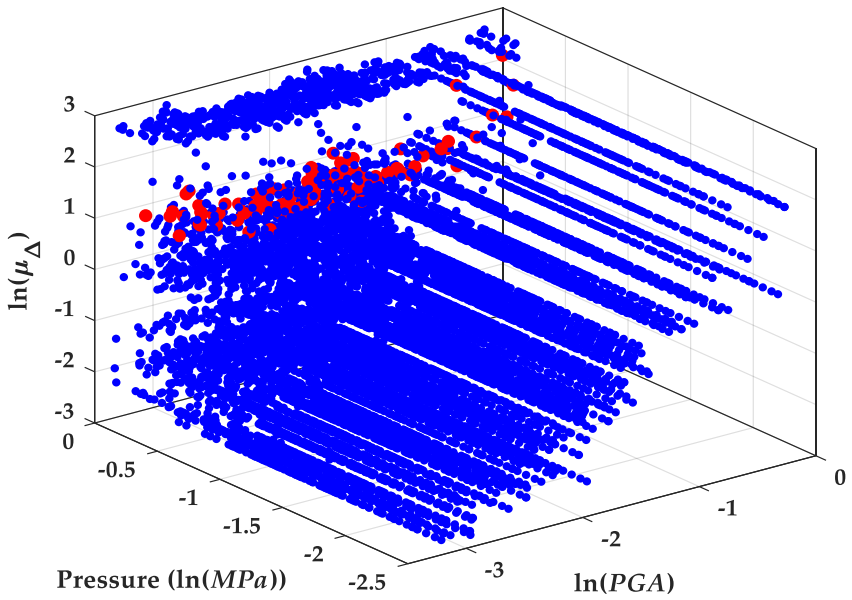

Figure 5: Response cloud due to varying seismic and landslide loadings.

Figure 6(a) shows the EDP–IM relationships for the as-built model under earthquake-only and combined loading, prior to incorporating slope failure probability. At lower IMs, the response is primarily driven by landslide pressure. Above a threshold—around a PGA of

0.45g—earthquake intensity dominates, and the structural response is governed by seismic loading alone. This threshold is defined by the landslide pressure acting on the pier. Figure 6(b) presents the EDP–IM relationships after incorporating slope failure probability. At lower IMs, structural response is mainly driven by seismic loading, as the likelihood of slope failure is low. A linear PSDM is then fitted to this relationship, where a noticeable increase in response is seen due to added landslide loading. This process can be repeated for other landslide intensities.

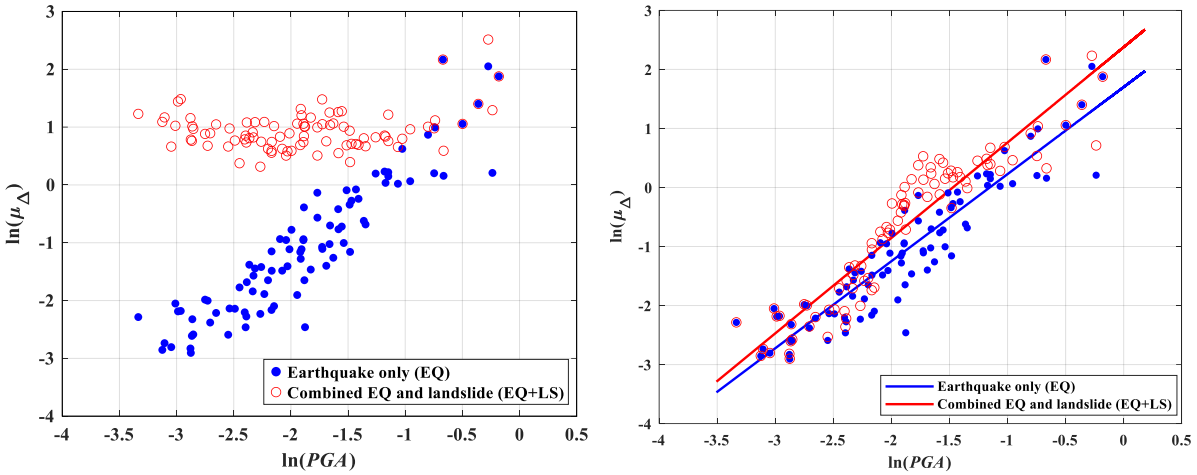

Figure 6: EDP-IM comparison of earthquake only and combined earthquake-landslide loading for non-corroded case; (a) Before applying slope failure probability; and (b) After applying slope failure probability and fitting linear PSDM.

4.3 Effect of corrosion rate and aging

Like the non-corroded case, PSDMs for various levels of corrosion are developed, depending on the corrosion rate and the considered years of service for the same landslide intensity as in the previous section. Table 2 displays the slope, intercept, and coefficient of determination (R^2) values of the linear regression conducted to formulate PSDMs for medium corrosion deterioration scenarios.

Table 2: Resulting PSDMs for medium corrosion case

Service Life (years) (t)		Intercept	Slope	R^2
Earthquake loading only	0	1.701	1.475	0.855
	25	1.776	1.505	0.846
	50	1.815	1.512	0.841
	75	1.964	1.567	0.824
Combined earthquake-landslide loading	0	2.378	1.616	0.876
	25	2.623	1.686	0.860
	50	3.171	1.821	0.768
	75	3.831	2.014	0.785

Figure 7(a) presents a graphical representation of the case at 75 years of service life across all corrosion rates. The findings indicate that a low corrosion rate does not cause any significant deterioration, and as the corrosion rate and time elapsed increase, the structural response also

intensifies. This outcome is expected, as the increasing corrosion rate and time elapsed lead to a reduction in the rebar area, consequently amplifying the response of the bridge pier.

To illustrate the impact of combined earthquake and landslide loading on the bridge's performance, a plot comparing the ductility response under earthquake-only loading (EQ) and combined earthquake and landslide loading (EQ+LS) for 25 years is presented in Figure 7(b). The comparison between EQ only and EQ+LS scenarios reveal that data points start to shift towards the EQ+LS side as the corrosion rate increases. This shift indicates higher structural responses due to the additional landslide loading, particularly in the highly corroded model. This trend demonstrates that even at 25 years of service, the combined effect of earthquake and landslide loading significantly influences the structural response of the bridge, emphasizing the importance of considering these combined effects in the design and maintenance of aging infrastructure.

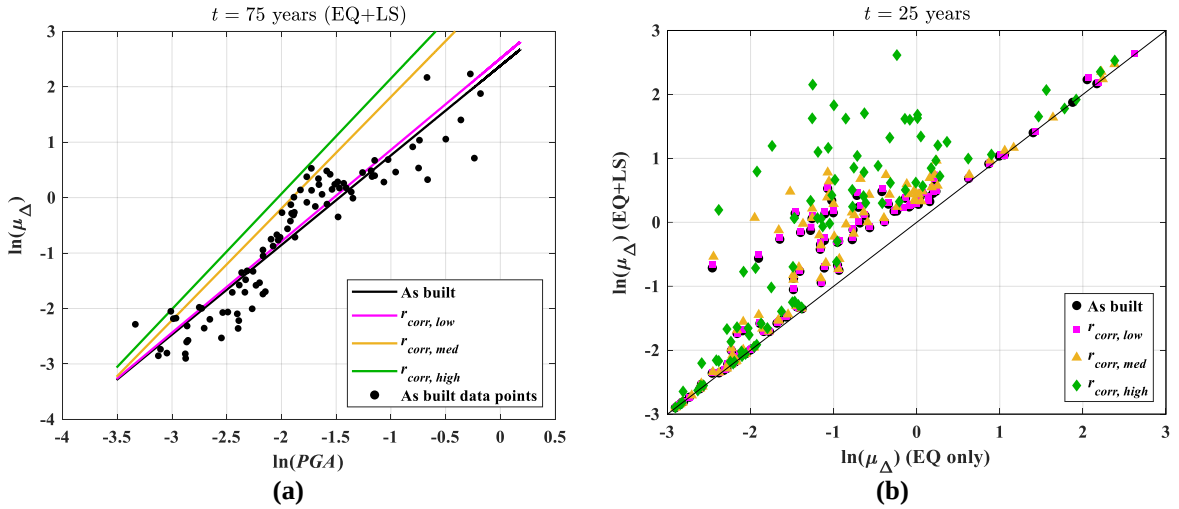

Figure 7: (a) PSDMs for 75 years of service for combined earthquake and landslide load; (b) Response comparison between earthquake only and combined earthquake and landslide loading across all corrosion rates and 25 years of service.

5 CONCLUSIONS

This study proposes an integrated methodology to assess the seismic response of aging highway bridges subjected to earthquake-induced flow-type landslides and corrosion. By combining advanced computational modeling with probabilistic analysis, the framework captures bridge behavior under varying deterioration and seismic conditions. It involves four main stages: landslide run-out analysis, displacement-based hazard assessment, nonlinear time-history analysis, and development of a modified probabilistic seismic demand model. The approach is applied to a case-study bridge, accounting for different levels of corrosion. The key findings are summarized below:

- The hysteretic response analysis reveals that corrosion significantly diminishes the force-resisting capacity of bridge columns, leading to higher displacements under seismic loading. When combined with landslide forces, especially in the direction of landslide flow, the structural response is much higher, resulting in significant damage to bridges with medium and high corrosion rates. This underscores the critical need to

account for both seismic and landslide forces in the design and maintenance of aging infrastructure to ensure resilience and safety.

- The combined earthquake and landslide load substantially affect the bridge pier performance, with the structural response heavily dependent on the ground motion's intensity.
- The probability of slope failure is a critical factor in determining the threshold at which landslide pressure becomes significant and leads to an increase in structural response compared to earthquake-only cases.
- The investigation reveals the significant impact of corrosion on bridge performance, with the corrosion rate and years of service directly affecting structural response. As corrosion rates and age of the bridge pier increase, structural response increases due to a reduction in rebar area, highlighting the importance of corrosion mitigation strategies in bridge maintenance and design.

These findings emphasize the importance of considering the combined effects of earthquakes and landslides, as well as corrosion deterioration, in the design and management of highway bridges in seismically active regions. Future research should focus on further refining the impact pressure models for flow-type landslides and exploring the sensitivity of structural responses to varying stand-off distances between the bridge site and landslide trigger locations. To support risk-informed decision-making, the development of fragility curves will be undertaken to capture the probabilistic response of bridges under combined seismic and landslide hazards. Additionally, incorporating uncertainties in landslide characteristics and soil properties will enhance the reliability of the proposed methodology.

REFERENCES

[1] Huang, R. Pei, X. Fan, X. Zhang, W. Li, S. Li, B. The characteristics and failure mechanism of the largest landslide triggered by the Wenchuan earthquake, May 12, 2008, China. *Landslides* (2012) **9**:131–142.

[2] Owen, L.A. Kamp, U. Khattak, G.A. Harp, E.L. Keefer, D.K. Bauer, M.A. Landslides triggered by the 8 October 2005 Kashmir earthquake. *Geomorphology* (2008) **94**:1–9.

[3] Hübl, J. Suda, J. Proske, D. Kaitna, R. Scheidl, C. Debris Flow Impact Estimation steep slopes. *International Symposium on Water Management and Hydraulic Engineering* (2009).

[4] Pang, Y. Meng, R. Li, C. Li, C. A probabilistic approach for performance-based assessment of highway bridges under post-earthquake induced landslides. *Soil Dynamics and Earthquake Engineering* (2022) **155**:107207.

[5] Haugen, E. Kaynia, A. Vulnerability of structures impacted by debris flow. In: *Landslides and Engineered Slopes. From the Past to the Future*. CRC Press; 2008:381–387.

[6] Jakob, M. Stein, D. Ulmi, M. Vulnerability of buildings to debris flow impact. *Natural Hazards* (2012) **60**:241–261.

[7] Mavrouli, O. Fotopoulou, S. Pitilakis, K. *et al.* Vulnerability assessment for reinforced concrete buildings exposed to landslides. *Bulletin of Engineering Geology and the Environment* (2014) **73**:265–289.

[8] Zeng, C. Cui, P. Su, Z. Lei, Y. Chen, R. Failure modes of reinforced concrete columns of buildings under debris flow impact. *Landslides* (2015) **12**:561–571.

[9] Parisi, F. Sabella, G. Flow-type landslide fragility of reinforced concrete framed buildings. *Eng Struct* (2017) **131**:28–43.
[10] Fotopoulou, S.D. Pitilakis, K.D. Fragility curves for reinforced concrete buildings to seismically triggered slow-moving slides. *Soil Dynamics and Earthquake Engineering* (2013) **48**:143–161.
[11] Andisheh, K. Scott, A. Palermo, A. Seismic Behavior of Corroded RC Bridges: Review and Research Gaps. *International Journal of Corrosion* (2016) **2016**:1–22.
[12] Alipour, A. Shafei, B. Shinozuka, M. Performance Evaluation of Deteriorating Highway Bridges Located in High Seismic Areas. *Journal of Bridge Engineering* (2011) **16**:597–611.
[13] ANSYS Inc. ANSYS® Academic Research Mechanical, Release 2020 R2. (2020).
[14] Uzuoka, R. Yashima, A. Kawakami, T. Konrad, J.M. Fluid dynamics based prediction of liquefaction induced lateral spreading. *Comput Geotech* (1998) **22**:243–282.
[15] Chen, H. Lee, C.F. Runout Analysis of Slurry Flows with Bingham Model. *Journal of Geotechnical and Geoenvironmental Engineering* (2002) **128**:1032–1042.
[16] Lee, K. Kim, Y. Ko, J. Jeong, S. A study on the debris flow-induced impact force on check dam with- and without-entrainment. *Comput Geotech* (2019) **113**:103104.
[17] Luo, H.Y. Zhang, L.L. Zhang, L.M. Progressive failure of buildings under landslide impact. *Landslides* (2019) **16**:1327–1340.
[18] Newmark, N.M. Effects of earthquakes on dams and embankments. *Geotechnique* (1965) **15**:139–160.
[19] Jibson, R.W. Regression models for estimating coseismic landslide displacement. *Eng Geol* (2007) **91**:209–218.
[20] Jibson, R.W. Harp, E.L. Michael, J.A. A method for producing digital probabilistic seismic landslide hazard maps. *Eng Geol* (2000) **58**:271–289.
[21] McKenna, F. Mazzoni, S. Scott, M. Fenves, G. Open system for earthquake engineering simulation. *University of California, Berkeley, CA* (2000).
[22] Cui, P. Zeng, C. Lei, Y. Experimental analysis on the impact force of viscous debris flow. *Earth Surf Process Landf* (2015) **40**:1644–1655.
[23] Alipour, A. Shafei, B. Performance Assessment of Highway Bridges Under Earthquake and Scour Effects. *15th World Conference of Earthquake Engineering* (2012) **18**.
[24] Thoft-Christensen, P. Assessment of the reliability profiles for concrete bridges. *Eng Struct* (1998) **20**:1004–1009.
[25] Cornell, C.A. Jalayer, F. Hamburger, R.O. Foutch, D.A. Probabilistic Basis for 2000 SAC Federal Emergency Management Agency Steel Moment Frame Guidelines. *Journal of Structural Engineering* (2002) **128**:526–533.
[26] Chawla, A. Chawla, S. Pasupuleti, S. Rao, A.C.S. Sarkar, K. Dwivedi, R. Landslide Susceptibility Mapping in Darjeeling Himalayas, India. *Advances in Civil Engineering* (2018) **2018**:1–17.
[27] Shekhar, S. Ghosh, J. Ghosh, S. Impact of Design Code Evolution on Failure Mechanism and Seismic Fragility of Highway Bridge Piers. *Journal of Bridge Engineering* (2020) **25**:1–19.